First-principles molecular dynamics modeling of the molten fluoride salt with Cr solute

H. O. Nam, A. Bengtson, K. Vörtler, S. Saha, R. Sakidja, D. Morgan*

Department of Materials Science and Engineering, University of Wisconsin-Madison, Madison, Wisconsin 53706, USA

ABSTRACT

Fluoride salts and their interactions with metals are of wide interest for the nuclear community. In this work, first-principles molecular dynamics (FPMD) was employed to study both pure molten fluoride salt and fluoride salt with dissolved solute Cr ions (a common corrosion product) at high temperature (823K–1423K). Two types of molten fluoride salts, namely flibe ($LiF\text{-}BeF_2$) and flinak (LiF-NaF-KF), with the Cr^0, Cr^{2+} and Cr^{3+} ions were chosen as a target system for the FPMD modeling. The prediction of thermo-kinetic properties of pure fluoride salt, such as the equilibrium volume, density, bulk modulus, coefficient of thermal expansion, and self-diffusion coefficient, provide useful extensions of existing data and verify the accuracy of the FPMD simulation in modeling of fluoride salts. The FPMD modeling of solute Cr in fluoride salt shows the effect of Cr valence on diffusivity and local structure in the salt.

*Corresponding author

Dane Morgan
Associate Professor,
Department of Materials Science and Engineering,
University of Wisconsin-Madison, Madison, Wisconsin 53706

Email: ddmorgan@wisc.edu

1. Introduction

Molten fluoride salt has been studied extensively as a coolant or a fuel salt for nuclear reactor systems because it can serve as an effective heat transfer fluid under high temperature, low pressure and high radiation flux conditions. In the late 1960s, Oak Ridge National Laboratory (ORNL) performed the molten salt reactor experiment (MSRE) to assess the potential application of molten fluoride salts for nuclear power reactor systems [1, 2]. During the operation of MSRE, the molten mixture of LiF-BeF_2 (denoted "FLiBe") with dissolved fuels was utilized as a primary coolant as well as a host for the fuel itself. Despite the fact that molten salt reactor technology has not been extensively researched thereafter, the molten salt reactor (MSR) system utilizing the fluoride salt as a coolant is still actively considered as one of the six major reactor concepts for Generation-IV technology [3]. Fluoride-cooled high-temperature reactor (FHR) [4, 5] and liquid fluoride thorium reactor (LFTR) [6] concepts that are being currently explored also propose the molten fluoride as a coolant or fuel salt, respectively. Furthermore, FLiBe has also been considered as a self-cooled tritium breeder in nuclear fusion reactor designs [7-9].

The major corrosion characteristics of candidate structural materials that are exposed to fluoride salts have been investigated quite extensively [10-17]. In general, molten fluoride salts are not considered corrosive to the structural materials because of the inherently high thermodynamic stability of the salt constituents' fluorides, which is greater than that of the binary fluorides of Cr, Fe and Ni, three major elemental constituents of the supporting steel structures. Nevertheless, the presence of excess fluorine in the fluoride salts can still be detrimental to the structural materials [14, 18, 19]. The behavior of Cr in fluoride salts is of particular interest, since amongst these three major constituents of the structural materials, chromium fluoride has the highest chemical activity and hence readily dissolved into the fluoride salts.

While there have been extensive thermo-kinetic properties of molten salts obtained in the 1960s, there continues to be a need to model of molten salts, both to validate the experimental data where there is significant scatter and also to generate the data when no experimental measurements were made. For these reasons, classical interatomic potential molecular dynamics (IPMD) has been used for modeling of various molten salt systems [20-22] including the flibe (FLiBe; Li_2BeF_4) [23-25] and flinak (FLiNaK; eutectic LiF-NaF-KF) [26-28] salts. Although there has been a slight variation in the forms of interatomic pair potentials used, the Tosi-Fumi (or Born-Huggins-Meyer) type potential [29-31] was typically used to model most of the molten salt systems. Parameters in these interatomic potentials were determined primarily by fitting the experimental and/or first-principles data.

In this work, instead of using interatomic potentials and IPMD, we employ first-principles molecular dynamics (FPMD) (also referred to as *ab-initio* molecular dynamics, or AIMD) directly to model the molten fluoride salt at high temperature. Due to the rapid growth of computer performance, FPMD can now be practically used in modeling of various liquid systems

[32-37], and has previously been applied to the flibe salt [38]. This previous work on flibe salt was conducted using the Car-Parrinello method [39], which is different with Born-Oppenheimer MD used in this study, and primarily focused on the diffusion at a fixed volume of $2g/cm^3$.FPMD has several advantages over IPMD, including the accuracy of full quantum mechanical calculation of the forces, the flexibility to study any system without needing to first fit potentials, and the ability to study electronic properties (e.g., spin state) that are not accessible to potentials.

In this paper, two representative fluoride salts for nuclear application were studied by using FPMD, with goals of both assessing FPMD for these salts and enhancing our knowledge of key thermodynamics and kinetic properties of the salts. The salts are flibe, which is considered as a primary coolant or fuel salt, and flinak, which is a candidate as a secondary coolant in fission reactor designs. Firstly, details of computational methods to model the molten fluoride salt systems through FPMD are addressed. Basic thermo-kinetic properties were calculated and compared with the experimental measurements to validate the FPMD modeling of fluoride salts. Then we focused on the modeling of the chromium solute interactions within the salt which is a major corrosion product of structural materials in fluoride salts at high temperature.

2. Computational methods

2.1 Details of first-principles molecular dynamics simulation

Initialization of the FPMD follows the approach from Bengtson et al. [37]. Initial configuration of ions for molecular dynamics was prepared by packing ions randomly in the simulation cell using Packmol package [40]. Then, IPMD simulation with the LAMMPS simulation package [41] was performed to obtain a reasonable input configuration of ions for FPMD. This step ensures the system to be at equilibrium before the FPMD simulation. Interatomic potential parameters for pure flibe and flinak were obtained from previous IPMD studies [23, 27] without taking Tang-Toennies dispersion damping term which can be replaced by a constant value of 1.0 [42]. The potential parameters between solute Cr and constituent elements of flibe and flinak salts were approximated following the method detailed in Larsen et al. [43]. We should note here that the IPMD simulation was merely employed as a preprocessing step to set up the initial configuration prior to the FPMD simulation, and thus the approximation of potential parameters should not affect the final results. Detailed procedures for geometry optimization using IPMD was addressed in the previous study [37]. After the IPMD runs, the molten state of the salt was verified by analyzing the radial distribution function (RDF) of atoms in the simulation cell. The RDF were compared with those reported in the literature data [24]. We consider simulation cells for flibe comprised of 28 Li atoms, 14 Be atoms, and 56 F atoms (total 98 atoms) and flinak comprised of 23 Li atoms, 6 Na atoms, 21 K atoms, and 50 F atoms (total 100 atoms). The cell

sizes are expected to be adequately converged with respect to the properties evaluated in this work based on a similar study on the Li-K-Cl system [37].

The FPMD simulations for molten fluoride salts have been performed with density functional theory (DFT) as implemented in the Vienna *Ab-Initio* Simulation Package (VASP) version 5.3.2 [44-46]. The molecular dynamics simulations are done in a statistical ensemble of fixed particle number, volume and temperature (NVT) using a Nosé-thermostat [47]. The Perdew-Burke-Ernzerhof (PBE) exchange-correlation functional was implemented in the generalized gradient approximation (GGA) [48, 49]. Dispersion forces are included using the vdW-DF method with the optB88 functional [50], as discussed in detail in Sec. 2.3. The calculations used projector augmented wave (PAW) technique and a plane wave basis set with an energy cutoff of 600eV [46, 51]. A 1×1×1 k-point mesh was chosen to be used in FPMD simulations, yielding an error of less than 1meV/atom with respect to k-points. Time step for the FPMD simulations were chosen at 0.001ps (1fs) to ensure an energy drift less than 1meV/atom-ps for pure salts and 2meV/atom-ps for solute systems.

FPMD simulations were performed for pure molten fluoride salts (flibe and flinak) at multiple simulation temperatures (T=973, 1223, 1423 K) to obtain a temperature dependent thermo-kinetic properties. To study the behavior of Cr solute in the salt, Cr atom, CrF_2 and CrF_3 molecules were introduced in the pure salt to simulate the behavior of Cr^0, Cr^{2+} and Cr^{3+} ion, respectively. When Cr solute is introduced into the salt, spin polarized calculations were conducted to accurately describe the effect of solute system. The pressure of the system at a finite temperature was determined by taking the sum of the external pressure and the kinetic pressure from the output of the VASP-MD. The standard error of the mean from correlated molecular dynamics data was determined from the auto-covariance function as can be found in the work of Alexopoulos [52].

2.2 Evaluation of thermo-kinetic properties from FPMD

The equation of state (EOS) analysis was conducted to determine pressure (P) vs. volume (V) for a series of volumes at a given temperature which were calculated from the FPMD simulations. The P(V) dependence is then fit to a third-order Birch-Murnaghan equation of state [53, 54] to obtain equilibrium volume, density and bulk modulus. From the temperature dependence of the density, coefficient of thermal expansion (CTE; α) was calculated using Eq. (1).

$$\alpha \equiv \frac{1}{V}\left(\frac{dV}{dT}\right)\Big|_P = -\frac{1}{\rho}\left(\frac{d\rho}{dT}\right)\Big|_P \tag{1}$$

where V is the volume, T the temperature, and ρ the density. The error in each property was estimated according to the standard error propagation method during the EOS analysis.

The self-diffusion coefficient was calculated from the slope of the mean squared displacement (Eq. (2) of the center of mass of atoms of the same type as a function of time, according to the well-established Einstein relation presented in Eq. (3).

$$MSD = \left\langle \frac{1}{N}\sum_{i=0}^{N}\left(r_i(t_0+dt)-r_i(t_0)\right)^2 \right\rangle = \frac{1}{N\cdot n_t}\sum_{i=0}^{N}\sum_{j=0}^{n_t}\left(r_i(t_j+dt)-r_i(t_j)\right)^2 \quad (2)$$

$$D = \frac{1}{6}\lim_{t\to\infty}\frac{d}{dt}\left(MSD\right) \quad (3)$$

In order to calculate the self-diffusion coefficient of constituent elements of fluoride salt, FPMD simulations were conducted at the equilibrium volume for more than 12,000 time steps (total 12 ps simulation) with about 100-atom simulation cell (98 atoms for flibe and 100 atoms for flinak) at the temperatures of 973 K, 1223 K, and 1423 K. Four equal size of blocks were used to estimate the standard error of the mean diffusivity using the block averaging method [55]. Details of this methods are addressed in the previous study [37].

The self-diffusion coefficient of solute Cr in fluoride salts was also calculated from the FPMD simulations at 973K. Unlike the case of the solvent constituents of the molten salts, the accuracy of the diffusion coefficient of Cr solute can be quite limited as in this case there is only one Cr atom/ion introduced into the simulation cell. Therefore, a longer simulation is necessary to isolate the diffusivities of Cr^{2+} and Cr^{3+} solutes in the salts. For longer simulations, we reduced the size of the cell to 63 atoms for flibe (18 Li, 9 Be, and 36 F atoms) and 52 atoms for flinak (12 Li, 3 Na, 11 K, and 26 F atoms). These systems sizes are small enough that one must be concerned with periodic cell size effects influencing the predicted Cr diffusivity. However, testing with IPMD showed that the effect of the reduced system size is negligible on the calculated Cr diffusion coefficients.

The radial distribution function analysis was conducted from the FPMD trajectory to study the local structure surrounding solute $Cr^0/Cr^{2+}/Cr^{3+}$ ions in fluoride salts. The first-shell coordination number of Cr with the surrounding F anion was estimated by integrating the radial distribution function from zero to the first minimum. We refer to the integral of the RDF as the neighbor function (Eq. (4))

$$N_{\alpha\beta}(r') = 4\pi\cdot\rho_\beta\cdot\int_0^{r'} r^2 g_{\alpha\beta}(r)\,dr. \quad (4)$$

where $g_{\alpha\beta}(r)$ is the RDF between species α and β, and ρ_β the average number density of species β.

2.3 Effect of xc-functional and dispersion

In DFT calculations, the exchange-correlation functional (xc-functional) is used to calculate the electron-ion interaction. It is known that the LDA (local density approximation) xc-functional underestimate the lattice constant of solid system about 1% and GGA overestimate the lattice constant about 1% [56]. In this study, three exchange-correlation functionals were tested, initially without introducing the dispersion interactions. Firstly, GGA/PBE without dispersion was used to estimate the equilibrium volume of molten salt at multiple temperatures and it overestimates the equilibrium volume by about 9% (18%) compared to the experimental V_0 from Janz [57] (Ignat'ev et al. [58]) (Fig. 1). Although the difference is quite large compared to errors in solids, this difference can be explained by low bulk modulus of liquid salt (~10GPa), which means that even small errors in energy can yield large errors in volume. The LDA without dispersion interaction was also tested at 973K and it gives an estimate of V_0 lower than any of the experimental data, as shown in Fig. 1. Only one simulation at 973K was conducted with the LDA xc-functional because introducing the dispersion will lower the estimation of V_0 further and LDA was already predicting a significantly too low a volume. The PBEsol exchange-correlation, which usually shows a good estimation of the lattice constant for solid systems, especially for alkali metals and alkali halides, was also tested without dispersion [59]. PBEsol gives a better estimation of the volume at multiple temperatures (about 3% (11%) larger than the V_0 from Janz [57] (Ignat'ev et al. [58]).

For the accurate prediction of thermo-kinetic properties, van der Waals (vdW) dispersion interaction was included in the FPMD modeling of molten salt systems. Although general density functional theory cannot describe the van der Waals dispersions, several methods have been developed to be used in first-principles modeling [50, 60]. For the VASP-MD simulations, currently (VASP version of 5.3.2) two different methods can be used to include the dispersion interaction. Those are the DFT-D2 of Grimme [61, 62] and vdW-DF of Langreth and Lundqvist et al [50, 63]. The DFT-D2 method adds a semi-empirical dispersion term, which can be described from a simple pair-wise force field, to the DFT energy. Parameters (C6 dispersion coefficient and vdW radii) used in this force field were empirically determined and provided for the elements up to the atomic number of Xe (atomic number = 54). The vdW-DF method, on the other hand, uses a non-local energy term which approximately accounts for the nonlocal electron-electron correlations. Fig. 1 also shows a comparison between two dispersion methods for flibe system with GGA/PBE functional at multiple temperatures. Although both methods are within the range of experimental measurements, we decided to use the vdW-DF method instead of DFT-D2 in this study, because the vdW-DF method is a non-empirical method and hence can describe elements without specifying pre-determined parameters.

By employing the van der Waals dispersion between atoms in FPMD simulations, the system pressure is decreased by more than 1GPa in flibe system and hence the equilibrium volume is decreased by about 9-13% compared to the V_0 estimates without dispersion interaction.

Therefore, PBEsol and LDA with the dispersion interaction will give a poor estimation of equilibrium volume for molten fluoride salts. This trend with dispersion interaction is also observed in molten LiCl-KCl system [37]. In this study, therefore, the vdW-DF method with PBE functional is used in FPMD modeling of molten fluoride salts. For the vdW-DF method, several different optimizations of exchange functional have been made up to date. Among these optimizations, the optB88 functional is chosen to be used to study the molten fluorides, because it provided a good estimate for the lattice constant for solid alkali halides in previous literature [50].

3. Results and discussions

3.1 Thermodynamic properties of pure fluoride salts

The aim of this section is to benchmark the FPMD simulations against known molten fluoride salt thermodynamic properties to the extent possible and also provide additional new thermodynamic data where experimental values are missing or unreliable.

3.1.1 Equilibrium volume, density and bulk modulus

The density is an essential and very useful thermodynamic property for fluoride salts. Several correlations for density vs. temperature for flibe and flinak have been developed from experimental measurements [19]. In order to obtain a correlation for density (density vs. temperature) from purely first-principles, equilibrium volumes (V_0) of molten salt system at various temperatures were determined from EOS calculations. Fig. 2 shows an example of the EOS analysis for flibe at 973K used in this study, performed as described in the Methods Section. The comparison of the EOS fit and the experimental data of Janz [57] and Ignat'ev et al. [58] shows that the predicted V_0 is within the range of the experimental measurements. The same procedure was applied to molten flibe and flinak salt systems at three different temperatures (T=973, 1223, 1423 K) and additionally at T=823K for flibe.

Fig. 3(a) and (c) show the equilibrium volume of flibe and flinak, respectively, including error bars as a function of temperature. Experimental equilibrium volumes for flibe were predicted from the correlation for density of Janz [57] and Ignat'ev et al. [58] (800K−1080K) from the literature [19]. For flinak, the three experimental correlations for density of Grele et al. (d1) [64, 65], Vriesema et al. (d2) [16, 66, 67] and Janz et al. (d3) [68] given within Sohal et al. [19] are shown in the figure for comparison. In addition, one correlation for density (d4) of flinak obtained from IPMD simulation [27] is also included for comparison.

From the predicted V_0, correlations for density of flibe and flinak were determined and compared with the experimental correlations for density as shown in Fig. 3(b) and (d), respectively. The

linear fit of the density versus temperature in Fig. 3(b) suggests a correlation for density of pure flibe from FPMD simulations for the temperature range from 823 K to 1423 K of

$$\rho\ [\mathrm{kg/m^3}] = 2374 - 0.3967 \cdot T[\mathrm{K}] \quad (5)$$

where ρ is the density, and T the temperature in Kelvin. The correlation for density of pure flinak from the FPMD simulations for the temperature range from 973K to 1423K is

$$\rho\ [\mathrm{kg/m^3}] = 2477 - 0.4895 \cdot T[\mathrm{K}] \quad (6)$$

As shown in Fig. 3(b) and (d), calculated densities of flibe and flinak from the FPMD simulations at 973K are in good agreement with the experiments. However, at higher temperature at 1423K, calculated densities seem to be slightly overestimated, because of the smaller density decrease as the temperature increases compared to the experiments. Detail discussion on the slope of density vs. temperature is addressed in Sec. 3.1.2.

From the third-order Birch-Murnaghan fit of pressure-volume data, bulk moduli as a function of temperature also can be predicted. Fig. 4 shows the trend of bulk modulus as a function of temperature. A decrease of bulk modulus with increaseing temperature, which is the typical trend of bulk modulus for solid salt, is observed [69]. Although experimental data for pure flibe does not exist, the bulk modulus of a LiF-BeF_2-ThF_4-UF_4 mixture, which was estimated from the experimental compressibility-temperature correlation, is used for comparison instead [70]. Predicted bulk modulus from the FPMD modeling is within the experimental error range of the LiF-BeF_2-ThF_4-UF_4 mixture.

3.1.2 Coefficient of thermal expansion

The calculated CTE of flibe at 973K from the FPMD simulations is $2.00 \pm 0.14 \times 10^{-4}$ (1/K). Experimental CTE values, which are calculated from the experimental correlations for density of Janz [57] and Ignat'ev et al. [58], are 2.52×10^{-4} (1/K) and 3.28×10^{-4} (1/K), respectively. The calculated CTE of flinak at 973K from the FPMD is $2.45 \pm 0.10 \times 10^{-4}$ (1/K). Experimental CTE values of flinak, which are calculated from the correlations for density from previous references within Sohal et al. [19], are summarized in Table 1. In general, the CTE values from the FPMD simulations are slightly smaller than that from the experiments. The source of this discrepancy is not clear but a smaller value of CTE compared to experiment when applying FPMD has also observed by Woodward et al. [36] for different liquid system.

3.2 Kinetic properties of pure fluoride salts

Self-diffusion coefficients of Li^+, Be^{2+} and F^- ions in flibe and Li^+, Na^+, K^+ and F^- ions in flinak

were analyzed from the FPMD simulations. The estimated self-diffusion coefficient of Li^+, Be^{2+}, and F^- ions in flibe are shown in Fig. 5. This figure shows the temperature dependence as described by the Arrhenius equation. Diffusivity of Li^+ and F^- in flibe were measured experimentally in a relatively low temperature range by Iwamoto et al. [71] and Ohmichi et al. [72]. The Arrhenius equations for Li^+ and F^- diffusion are taken from the above references and plotted in the same figure for comparison. Due to the lack of experimental data of diffusivity in flibe, diffusivity of Li and F ions in flinak is added for comparison and discussion (Umesaki et al. [73]). The estimated self-diffusion coefficients for constituent ions of fluoride salts at multiple temperatures are summarized in Table 2.

In case of the Li^+ diffusion in flibe, the calculated diffusion coefficients are lower than the experimental value from Iwamoto et al. [71]. However, it should be noted that experimental diffusion coefficient of Li and F in flibe has an error range due to the spread of measured values [71, 72] and the FPMD results for Li diffusion in this study are close to the lower bound of the experimental Li diffusion in flibe. Although the measured diffusivity of Li in flibe and flinak differs in magnitude, the activation energies (slope of the Arrhenius plot) for the diffusion of Li in both flibe (solid line) and flinak (dashed line) are almost identical, and the activation energy from our study for Li diffusion is also very similar. Overall, this comparison suggests that our Li diffusion results are in good agreement with flibe and trends from flibe and flinak.

Unlike the Li case, the measured F^- diffusion in flibe shows much larger activation energy compared to that of F^- diffusion in flinak and the FPMD value of F^- diffusion in flibe. Ohmichi et al. [72] suggested either the exchange of fluorine atoms between neighboring beryllate anions (BeF_4^{2-}) or the F^- diffusion by means of a neutral ion pair (LiF) as a possible mechanism of F^- diffusion in flibe to explain the large value of the fluorine diffusion coefficient. However, the apparently extraordinarily high measured diffusivity of F ions in flibe has not yet been clearly explained. Because another measurement of F diffusion in flibe has not been made, it is difficult to conclude if the experiments might have an error. However, given the success of the FPMD for Li^+ in flibe, there is no reason to expect a significant error form the FPMD for F^- diffusion. Furthermore, the values for F^- diffusivities from FPMD are similar in both magnitude and activation energy to those in flinak (shown in Fig. 5) and NaF-AlF_3 [74] (not shown). These results, taken together, suggest that the values for F^- seen by Ohmichi, et al. [72] may contain errors and should be reevaluated.

Klix et al. used the Car-Parrinello MD to study the tritium diffusion in molten flibe and calculated the diffusion coefficients of lithium and fluorine [38]. The magnitude of the diffusion coefficients and the activation energies (slope of the data points) are consistent with the values from this study.

Diffusivities of Li^+, Na^+, K^+, and F^- ions in flinak were also determined in this work by FPMD, as shown in Fig. 6. The experimental diffusivities of constituent ions in flinak from Umesaki et

al. [73] are plotted in Fig. 6 for comparison. The values of activation energy for each ion are difficult to compare quantitatively to those obtained from experiments due to the relatively large error bars of each data point. In particular, since only six atoms of Na exist in the 100-atom cell for flinak, the error on the diffusivity of the Na ion is understandably greater than the others. However, estimated diffusivities of Li^+, Na^+, K^+, and F^- in flinak from FPMD simulations are in general agreement with those from the experimental results, especially at lower temperatures (note that the y-axis range in Fig. 6 is only about one order of magnitude).

As shown in Table 2, estimated diffusion coefficients of constituent ions of flinak (Li^+, Na^+, K^+, and F^-) were similar to each other within the error bars. In contrast, the diffusivities of Li^+ and F^- in flibe, which are common elements in both salts, show quite a significant difference between each other, with Li^+ being the fastest ion. It is possible that in flibe Be^{2+}, which has a higher valence state than any cations in flinak, interacts with the F^- and effectively forms a fluoro-beryllate anion (BeF_4^{2-}) which consequently slows the diffusion of the fluorine in flibe.

3.3 Behavior of Cr solute in molten fluoride salts

It is well known that chromium has two dominant oxidation states when it is dissolved in the salt. In cases when the Cr is dissolved in flibe, Cr(II) is the predominant oxidation state, but when the Cr is dissolved in flinak, Cr(III) is more stable [15]. Therefore, we considered both oxidation states of solute Cr in the salt. To assess the effect of different oxidation states of Cr solute, we introduced Cr, CrF_2 and CrF_3 into the salt to yield Cr^0, Cr^{2+} and Cr^{3+} solutes, respectively, within the salt.

3.3.1 Diffusion of Cr ions in molten fluoride salts

Self-diffusion coefficient of solute Cr in fluoride salts at 973K was calculated from the FPMD simulations. For these Cr solute containing systems, relatively smaller system sizes than the pure salts (63 atoms for flibe (18 Li, 9 Be, and 36 F atoms) and 52 atoms for flinak (12 Li, 3 Na, 11 K, and 26 F atoms)) were used to enable longer simulations (see Sec. 2.2 for more details).

To obtain reliable statistical averages of the self-diffusion coefficient of the Cr solute ion in the salt, nine independent FPMD simulations for 8ps were performed for each solute system. Then, the slopes of nine independent MSDs for each ion were averaged to determine the diffusion coefficient of Cr ion. The error in the Cr diffusivity was obtained by evaluating the standard error of the mean from these nine independent simulations. As shown in Fig. 7, FPMD is sensitive to the role of charge state of solute ions in flibe. The neutral atom moves faster than the charged solute ion, which interact more with the surrounding F^- ions. In flibe the Cr^{3+}, which exhibits a stronger bonding with surrounding F^- ions, also shows a smaller diffusion coefficient than that of the Cr^{2+} ion, as expected. However, this trend is not clear in flinak, where the

diffusion of Cr^{2+} and Cr^{3+} are not distinguishable within the error bars of our present calculation. The reason that the expected trend of lower diffusivity with higher valence is found with Cr in flibe but not in flinak is not clear at this time.

3.3.2 Structure around the Cr solute

Fig. 8 shows the radial distribution function (RDF) of flibe with Cr (solid lines), CrF_2 (dash-dot lines) and CrF_3 (short-dash lines), and calculated first-peak distances and first-shell coordination numbers for Cr, Cr^{2+} and Cr^{3+} in flibe and flinak are shown in Table 4. RDF curves between Be-F and Li-F are similar for all Cr valence states and the RDF between Be and Be (green lines) are affected only slightly by changing Cr valence. However, the Cr-F RDFs (orange lines) vary considerably due to the change in the valence state of Cr in the molten salts. When comparing the Cr^0-F, Cr^{2+}-F, and Cr^{3+}-F RDFs it is seen that the first peak increases and occurs at a small radius with increasing Cr charge. This trend indicates that the Cr ion has stronger bond with F ion when the Cr has a higher oxidation state, as expected. This trend is also supported by evaluating the first-shell coordination number of Cr with the surrounding F anion which can be estimated by integrating the radial distribution function (gray lines in Fig. 8) from zero to the first minimum. Similar trends to those observed here are also found in flinak.

The local structure of Cr solute in flibe salt was studied by analyzing the first-principles molecular dynamics simulation trajectory. The VMD program [75] was used to visualize the trajectory of FPMD simulation. Fig. 9 shows snapshots of FPMD trajectory of flibe system with the dissolved Cr solute. Both Fig. 9(a) and Fig. 9(b) were captured from the FPMD trajectory of flibe with Cr^{2+} system. For the Cr^{2+} ion one can observe various coordination polyhedral, such as a distorted square-planar (Fig. 9(a)) and octahedral (Fig. 9(b)) first-neighbor F^- shell. However, the Cr^{3+} ion in flibe makes a more stable octahedral Cr and F bonding structure, as can be seen in Fig. 9(c). This trend is also supported qualitatively by the slope of the $N(r)$ curves in Fig. 8, where the stable first-neighbor F- shell for Cr^{3+} leads to an $N(r)$ with a clear plateau while the less stable F- shell for Cr^{2+} leads to an to an $N(r)$ that never levels out. The first neighbor shell can be evaluated quantitatively by the coordination number between Cr and F in Table 4, which shows the value of 5.9 for Cr^{3+}, a value within the simulation uncertainties of the perfect octahedral coordination value of 6. The stability of more octahedrally coordinated Cr when in 3+ vs. 2+ state is consistent with its smaller size and larger valence, which is likely to attract F^- more strongly. The same analysis as performed for flibe was performed for the Cr^{2+} and Cr^{3+} in flinak and it shows a similar trend as for flibe.

The spin state of the Cr^{2+} and Cr^{3+} ions in molten salts were monitored during the FPMD simulations. Cr^{2+} and Cr^{3+} are d^4 and d^3 ions, with 4 and 3 d-orbital valence electrons, respectively. In fluoride salts, solute Cr^{2+} and Cr^{3+} have magnetic moments of four and three, respectively, which are the expected moments for their high spin states.

4. Conclusions

In this work, first-principles molecular dynamics (FPMD) modeling was employed to predict thermo-kinetic properties of two types of molten fluoride salts, flibe and flinak, and to assess the Cr solute behavior within the salts. The GGA/PBE exchange-correlation-functional (xc-functional) was used in the FPMD modeling, taking into account the van der Waals (vdW) dispersion interaction. The selection of the exchange-correlation functional and the method for the vdW dispersion was found to have a large influence on the equilibrium properties of the molten salt system.

The thermo-kinetic properties of pure fluoride salts such as the equilibrium volume, density, bulk modulus, coefficient of thermal expansion, and self-diffusion coefficient were predicted and compared to the experimental data or computational data. The predicted thermo-kinetic properties were generally in good agreement with the previous experimental literature, supporting the validity of FPMD simulation in modeling the fluoride salts at high temperatures. The FPMD was also used to generate data to validate the experimental data in cases where the data had a large scatter (e.g., different correlations for density vs. temperature, and F^- diffusion in flibe and flinak) and where no experimental measurements were available (e.g., bulk modulus, Be^{2+} diffusion in flibe, and Cr ions diffusion in flibe and flinak).

The FPMD modeling is well suited to studying impurities, as no potential fitting is needed to include them in the model. The self-diffusion coefficients for Cr were shown to be dependent on the oxidation state of the dissolved Cr ions, with higher valence Cr ions generally move slower. Further structural analysis on the Cr^{2+} and Cr^{3+} showed that Cr^{3+} was generally surrounded by ~6 F^- ions in a nearest-neighbor octahedral-like cage, while Cr^{2+} is located in various local structures including distorted square planar and octahedral type environments, with an average coordination number of ~5 F^- in its first neighbor shell. Cr was found to remain robustly in its high-spin states, with moments of 4 and 3 for Cr^{2+} and Cr^{3+}, respectfully.

This study demonstrates that FPMD can be used as a versatile tool to model fluoride molten salts and to study the behavior of dissolved solutes with varying valence states. Overall, by using FPMD, we have been able to provide new insights into the thermo-kinetic properties of flibe and flinak fluoride salts and Cr solutes in these salts.

Acknowledgements

This research was performed using funding received from the DOE Office of Nuclear Energy's Nuclear Energy University Programs (NEUP 10-100). The authors acknowledge the Extreme Science and Engineering Discovery Environment (XSEDE), which is supported by National Science Foundation grant number OCI-1053575. The authors also thank Christopher Woodward, who provided advice on running first-principles molecular dynamics simulations, including the addition of the kinetic energy term in VASP-MD.

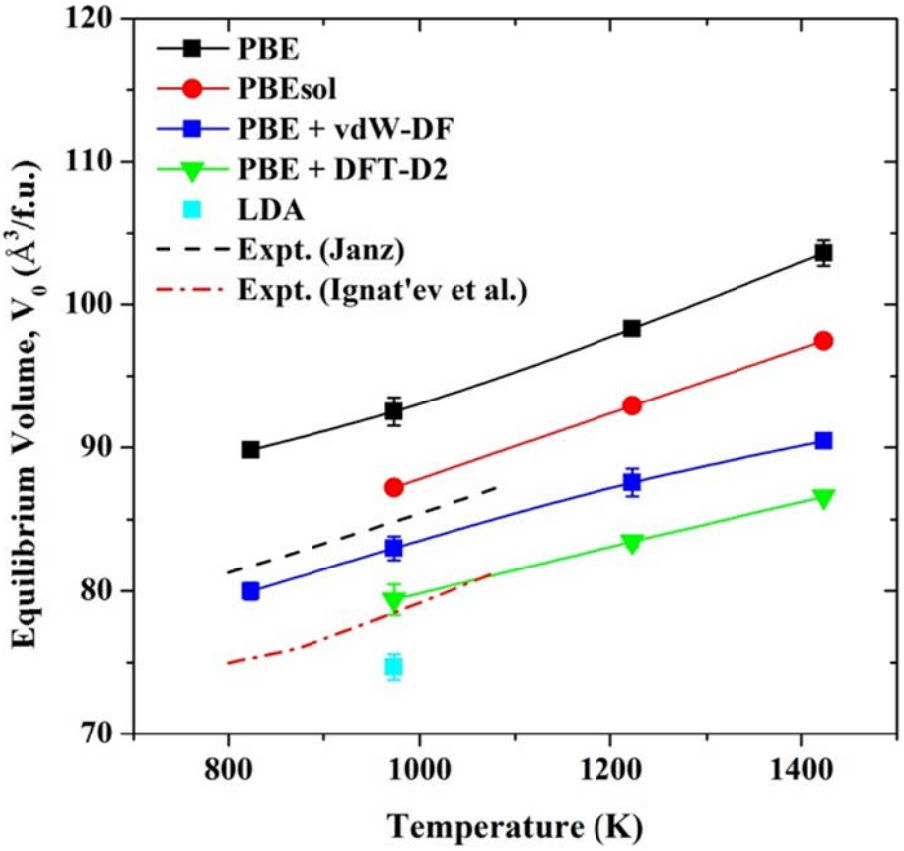

Fig. 1. Calculated equilibrium volume of flibe from the FPMD simulations as a function of temperature with different exchange-correlation functionals and with different dispersion methods. Experimental correlations for density of Janz [57]and Ignat'ev et al. [58] for flibe salt from literature [19] are shown together for comparison. Error bars represent two sigma standard error of the mean.

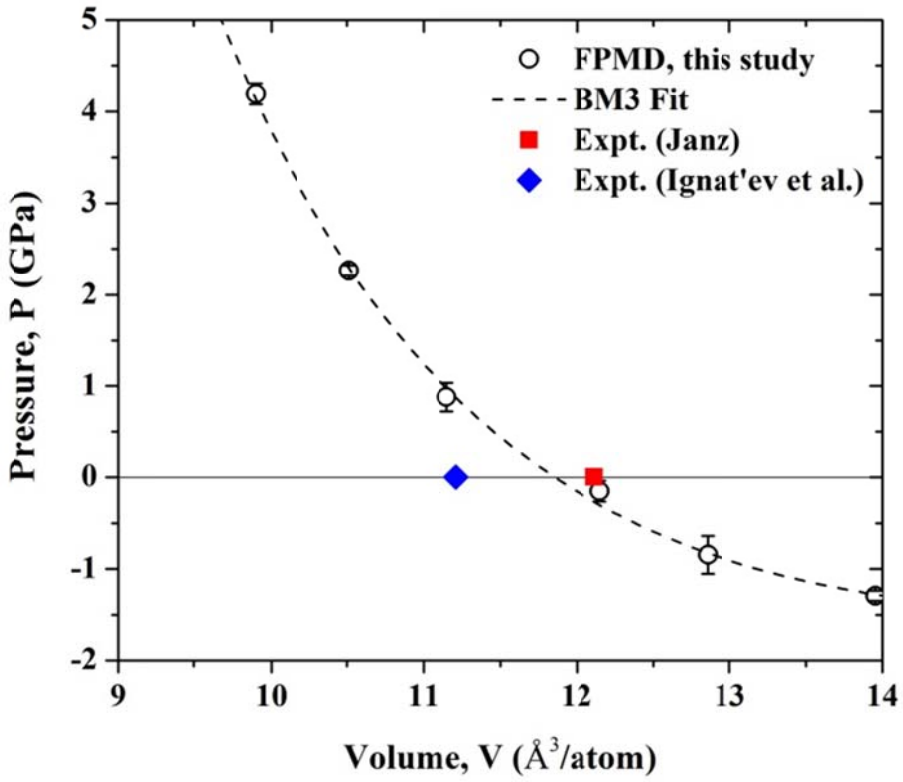

Fig. 2. The third-order Birch-Murnaghan equation of state fit of pressure-volume data of flibe at 973K which was obtained from the FPMD simulations. Experimental V_0 are also shown for comparison. Error bars represent one sigma standard error of the mean.

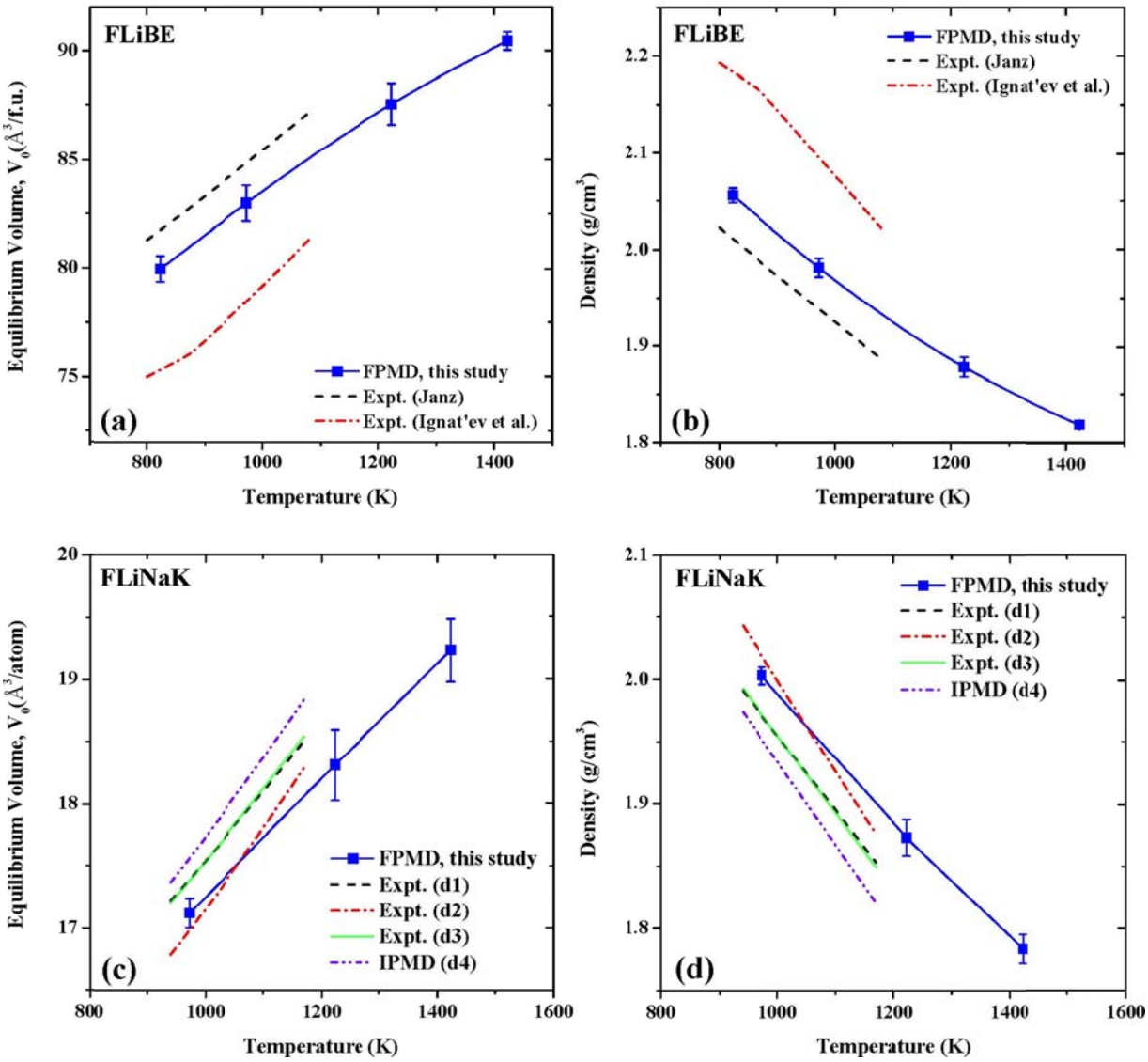

Fig. 3. Comparisons of the estimated equilibrium volume for (a) flibe and (c) flinak from the FPMD simulations with the experimental data and converted correlations for density for (b) flibe and (d) flinak. Experimental correlations for density of Janz and Ignat'ev et al. for flibe, and Grele IPMD density model for flinak (d4) [27] was added for comparison. Error bars represent two sigma standard error of the mean.

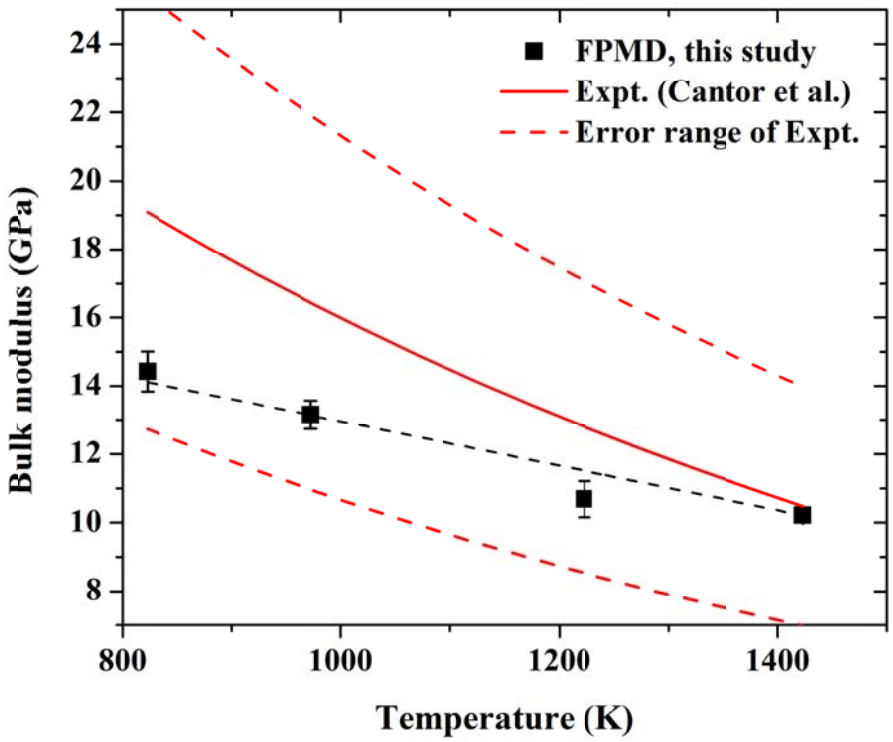

Fig. 4. Predicted bulk moduli (B) of flibe with errors at multiple temperatures. Bulk moduli were obtained from EOS fits as described in the Methods Section. Experimental bulk moduli were estimated from the compressibility-temperature correlation for LiF-BeF_2-ThF_4-UF_4 mixture [70]. Error bars represent one sigma standard error of the mean.

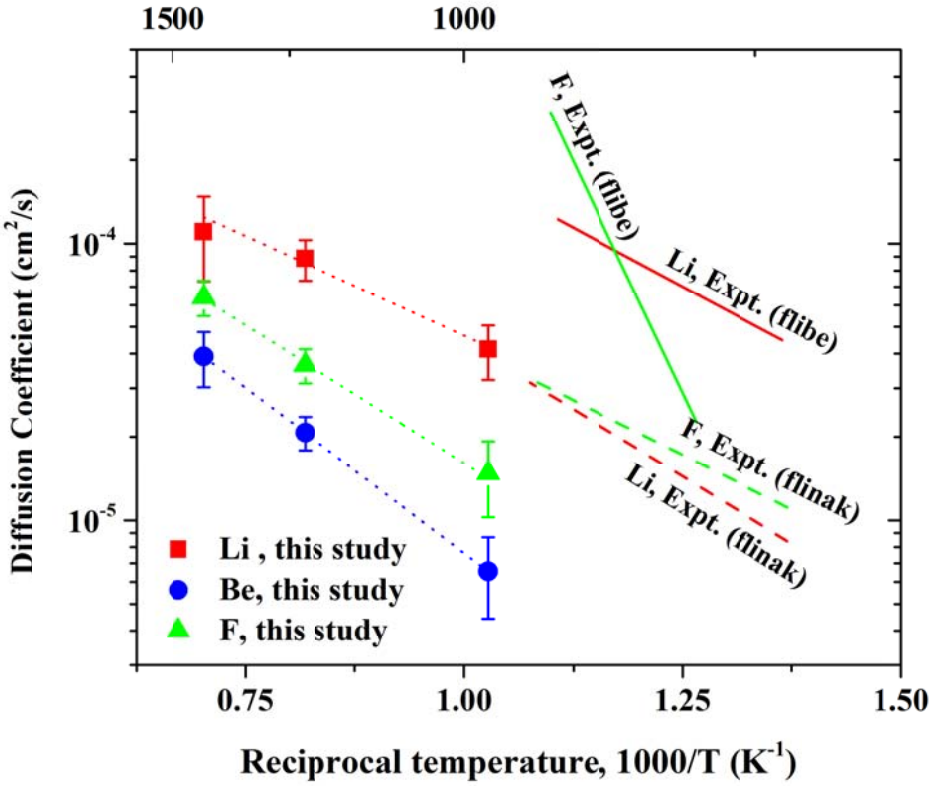

Fig. 5. Temperature dependence of self-diffusion coefficients of Li^{+}, Be^{2+} and F^{-} in flibe with error bar. Data points were obtained from the FPMD calculations at the temperatures of 973, 1223, and 1423K. Experimental diffusivity for Li and F are shown together for comparison [71-73]. Error bars represent one sigma standard error of the mean.

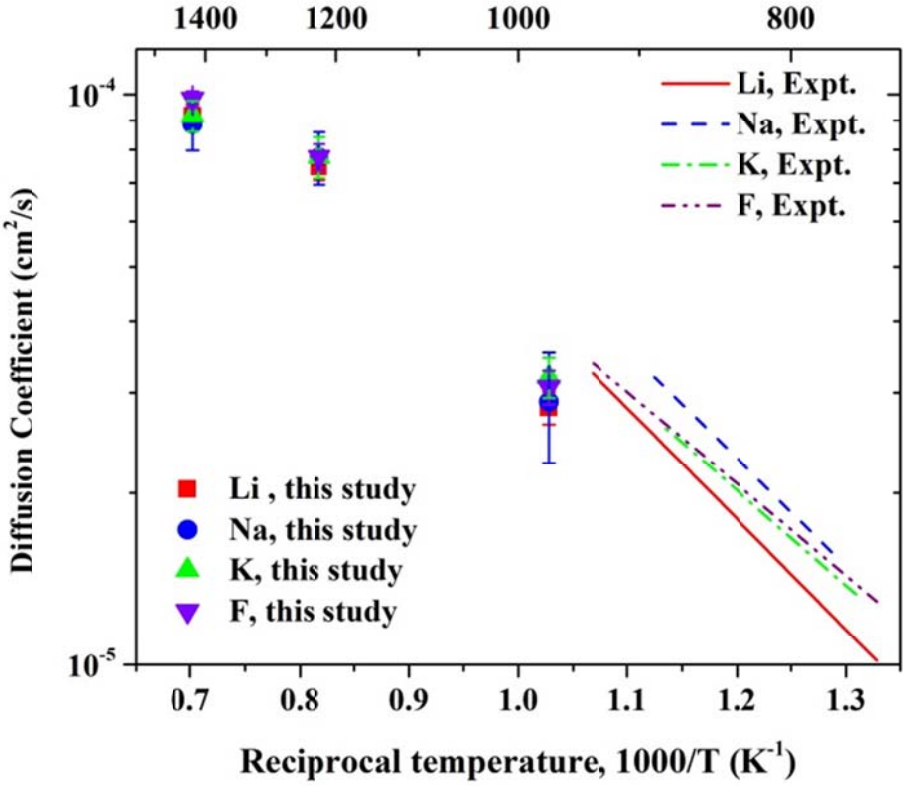

Fig. 6. Temperature dependence of self-diffusion coefficient of Li^+, Na^+, K^+ and F^- ions in flinak with error bar. Data points were obtained from the FPMD calculations at the temperatures of 973, 1223, and 1423K. The experimental values are added for comparison [73]. Error bars represent one sigma standard error of the mean.

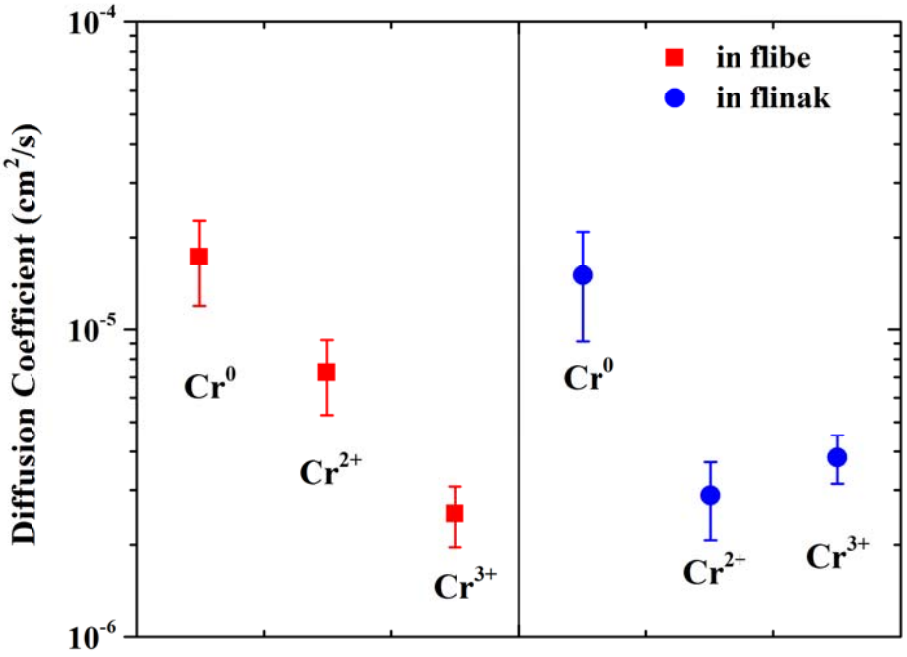

Fig. 7. Self-diffusion coefficients of solute Cr ions in flibe and flinak at 973K. Error bars represent one sigma standard error of the mean.

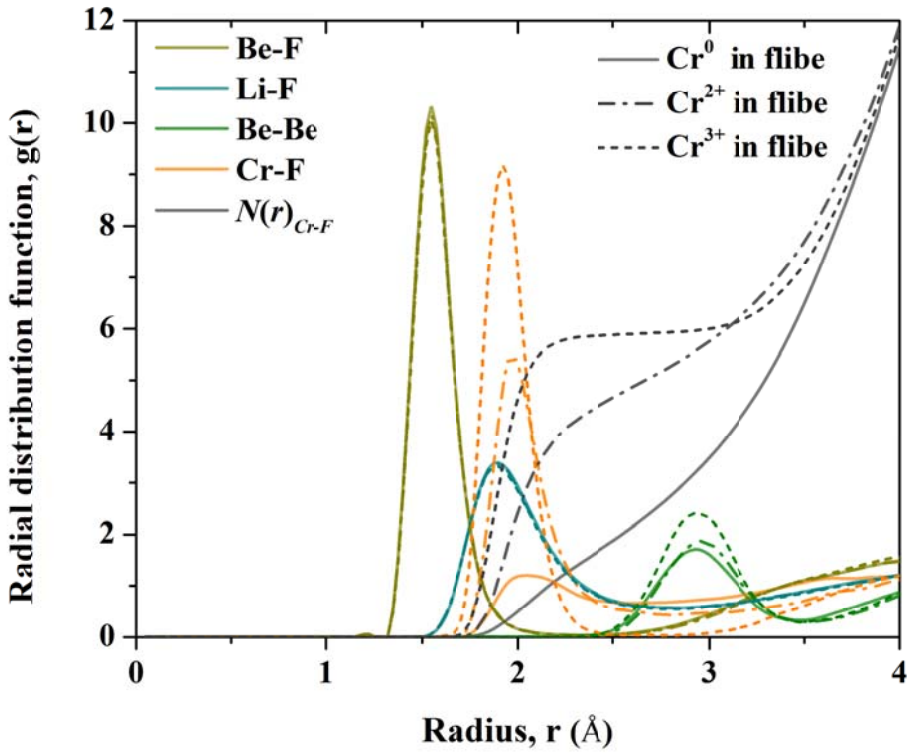

Fig. 8. Radial distribution functions (RDF) of flibe (98 total atoms) with CrF_2 and CrF_3. Solid lines denote the RDFs when Cr^0 is introduced into flibe. Dash-dot lines and short-dash lines denotes when CrF_2 and CrF_3 is introduced into flibe, respectively. Neighbor function, $N(r)$, between $Cr^0/Cr^{2+}/Cr^{3+}$ and F^- (gray lines) as defined in Sec. 2.2 are shown together.

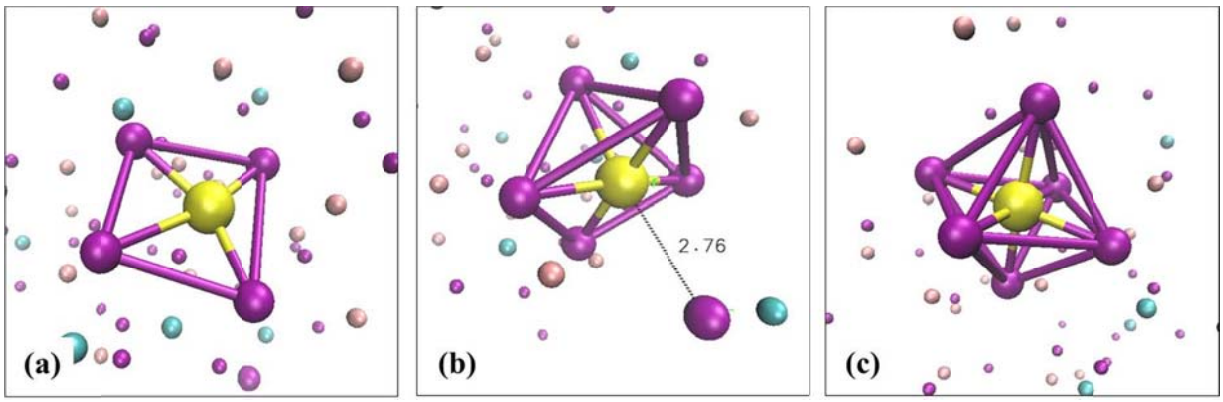

Fig. 9. Snapshots of FPMD trajectory for flibe with the solute Cr. Yellow ball is chromium ion and purple balls are fluorine ions. Pink balls and cyan balls are Li and Be, respectively. (a) FPMD snapshot of flibe with CrF_2 showing flat bonding between Cr and F; (b) FPMD snapshot of flibe with CrF_2 showing unstable octahedral structure of Cr and F; (c) FPMD snapshot of flibe with CrF_3 showing stable octahedral structure of Cr and F.

Table 1. Estimated coefficient of thermal expansion (CTE) of flibe and flinak at 973K from FPMD simulations and comparison with the CTEs from literature.

	FPMD, this study (1/K)	From literature (1/K)	References
CTE of flibe	$2.00 \pm 0.14 \times 10^{-4}$	2.52×10^{-4}	Janz [57]
		3.28×10^{-4}	Ignat'ev et al. [58]
CTE of flinak	$2.45 \pm 0.10 \times 10^{-4}$	3.04×10^{-4}	(d1) [64, 65]
		3.62×10^{-4}	(d2) [16, 66, 67]
		3.16×10^{-4}	(d3) [68]
		3.43×10^{-4}	(d4) [27]

Table 2. Estimated self-diffusion coefficients for constituent ions of flibe and flinak salt at multiple temperatures from the FPMD simulations. Error bars represent one sigma standard error of the mean.

Salt	Ions	Self-diffusion coefficient ($cm^2/s \times 10^{-5}$)		
		973K	1223K	1423K
Flibe	Li^+	4.14 ± 0.92	8.84 ± 1.48	11.1 ± 3.74
	Be^{2+}	0.65 ± 0.21	2.07 ± 0.29	3.91 ± 0.88
	F^-	1.48 ± 0.45	3.64 ± 0.52	6.41 ± 0.93
Flinak	Li^+	2.82 ± 0.19	7.47 ± 0.39	9.17 ± 0.46
	Na^+	2.89 ± 0.64	7.76 ± 0.82	8.87 ± 0.89
	K^+	3.20 ± 0.26	7.78 ± 0.64	9.18 ± 0.57
	F^-	3.07 ± 0.21	7.77 ± 0.42	9.83 ± 0.31

Table 3 Estimated self-diffusion coefficients for solute Cr ions in flibe and flinak at 973K from the FPMD simulations.

Salt	Ions	Self-diffusion coefficient ($cm^2/s \times 10^{-5}$)
Flibe	Cr^0	1.73 ± 0.54
	Cr^{2+}	0.73 ± 0.20
	Cr^{3+}	0.25 ± 0.06
Flinak	Cr^0	1.50 ± 0.58
	Cr^{2+}	0.29 ± 0.08
	Cr^{3+}	0.38 ± 0.07

Table 4. First-peak radius and first-shell coordination numbers for $Cr^0/Cr^{2+}/Cr^{3+}$ and F^- pairs in flibe and flinak. First shell coordination numbers are determined by the integral of the RDF up to its first minimum.

Salt	Ion pair	First-peak radius (Å)	Coordination number
Flibe	$Cr^0 – F^-$	2.05	2.1
	$Cr^{2+} – F^-$	1.97	5.2
	$Cr^{3+} – F^-$	1.93	5.9
Flinak	$Cr^0 – F^-$	1.97	2.7
	$Cr^{2+} – F^-$	1.96	4.9
	$Cr^{3+} – F^-$	1.94	5.9

References

[1] P.N. Haubenre, J.R. Engel, Nuclear Applications and Technology, 8 (1970) 118-136.

[2] M.W. Rosenthal, P.R. Kasten, R.B. Briggs, Nuclear Applications and Technology, 8 (1970) 107-118.

[3] U.S. DOE Nuclear Energy Research Advisory Committee and the Generation IV International Forum, A Technology Roadmap for the Generation IV Nuclear Energy Systems, GIF-002-00, 2002.

[4] C.W. Forsberg, Nuclear Technology, 144 (2003) 289-302.

[5] S. Greene, in: ICENES-2011, San Francisco, CA, 2011.

[6] R. Hargraves, R. Moir, American Scientist, 98 (2010) 304-313.

[7] D.A. Petti, G.R. Smolik, M.F. Simpson, J.P. Sharpe, R.A. Anderl, S. Fukada, Y. Hatano, M. Hara, Y. Oya, T. Terai, D.K. Sze, S. Tanaka, Fusion Engineering and Design, 81 (2006) 1439-1449.

[8] R.W. Moir, R.L. Bieri, X.M. Chen, T.J. Dolan, M.A. Hoffman, P.A. House, R.L. Leber, J.D. Lee, Y.T. Lee, J.C. Liu, G.R. Longhurst, W.R. Meier, P.F. Peterson, R.W. Petzoldt, V.E. Schrock, M.T. Tobin, W.H. Williams, Fusion Technology, 25 (1994) 5-25.

[9] T. Terai, Y. Hosoya, S. Tanaka, A. Sagara, O. Motojima, Journal of Nuclear Materials, 258–263, Part 1 (1998) 513-518.

[10] J.H. DeVan, Transactions of the American Nuclear Society, 46 (1984) 210-211.

[11] M. Kondo, T. Nagasaka, T. Muroga, A. Sagara, N. Noda, Q. Xu, D. Ninomiya, N. Masaru, A. Suzuki, T. Terai, Fusion Science and Technology, 56 (2009) 190-194.

[12] M. Kondo, T. Nagasaka, A. Sagara, N. Noda, T. Muroga, Q. Xu, M. Nagura, A. Suzuki, T. Terai, Journal of Nuclear Materials, 386-88 (2009) 685-688.

[13] M. Kondo, T. Nagasaka, Q. Xu, T. Muroga, A. Sagara, N. Noda, D. Ninomiya, M. Nagura, A. Suzuki, T. Terai, N. Fujii, Fusion Engineering and Design, 84 (2009) 1081-1085.

[14] L.C. Olson, in: Thesis, Nuclear Engineering, University of Wisconsin-Madison, 2009.

[15] D.F. Williams, L.M. Toth, in: ORNL/GEN4/LTR-05-011, Oak Ridge National Laboratory, 2005.

[16] D.F. Williams, L.M. Toth, K.T. Clarno, in: ORNL/TM-2006/12, Oak Ridge National Laboratory, 2006.

[17] K. Sridharan, M. Anderson, M. Corradini, T. Allen, L. Olson, J. Ambrosek, D. Ludwig, in: NERI Final Report, University of Wisconsin, Madison, WI, July 9, 2008, 2008.

[18] B. Laurenty, in: Thesis, Nuclear Engineering, University of California Berkeley, 2006.

[19] M.S. Sohal, M.A. Ebner, P. Sabharwall, P. Sharpe, in, Idaho National Laboratory, 2010.

[20] C. Caccamo, M. Dixon, Journal of Physics C: Solid State Physics, 13 (1980) 1887.

[21] F. Lantelme, P. Turq, The Journal of Chemical Physics, 77 (1982) 3177-3187.

[22] M. Wilson, P.A. Madden, Journal of Physics: Condensed Matter, 5 (1993) 2687.

[23] R.J. Heaton, R. Brookes, P.A. Madden, M. Salanne, C. Simon, P. Turq, The Journal of Physical Chemistry B, 110 (2006) 11454-11460.

[24] M. Salanne, C. Simon, P. Turq, R.J. Heaton, P.A. Madden, The Journal of Physical Chemistry B, 110 (2006) 11461-11467.

[25] B. Jabes, M. Agarwal, C. Chakravarty, J Chem Sci, 124 (2012) 261-269.

[26] M. Matsumiya, R. Takagi, Electrochimica Acta, 46 (2001) 3563-3572.

[27] M. Salanne, C. Simon, P. Turq, P.A. Madden, Journal of Fluorine Chemistry, 130 (2009) 38-44.

[28] C. Merlet, P.A. Madden, M. Salanne, Physical Chemistry Chemical Physics, 12 (2010) 14109-14114.

[29] M.L. Huggins, J.E. Mayer, The Journal of Chemical Physics, 1 (1933) 643-646.

[30] F.G. Fumi, M.P. Tosi, Journal of Physics and Chemistry of Solids, 25 (1964) 31-43.

[31] M.P. Tosi, F.G. Fumi, Journal of Physics and Chemistry of Solids, 25 (1964) 45-52.

[32] D. Alfè, M.J. Gillan, Physical Review Letters, 81 (1998) 5161-5164.

[33] H.Z. Fang, W.Y. Wang, P.D. Jablonski, Z.K. Liu, Physical Review B, 85 (2012) 014207.

[34] P. Ganesh, M. Widom, Physical Review Letters, 102 (2009) 075701.

[35] B.B. Karki, D. Bhattarai, L. Stixrude, CMC-Comput. Mat. Contin., 3 (2006) 107-117.

[36] C. Woodward, M. Asta, D.R. Trinkle, J. Lill, S. Angioletti-Uberti, Journal of Applied Physics, 107 (2010) 113522-113510.

[37] A. Bengtson, S. Saha, H.O. Nam, R. Sakidja, D. Morgan, First-principles molecular dynamics modeling of the LiCl-KCl molten salt system (*submitted*), (2013).

[38] A. Klix, A. Suzuki, T. Terai, Fusion Engineering and Design, 81 (2006) 713-717.

[39] R. Car, M. Parrinello, Physical Review Letters, 55 (1985) 2471-2474.

[40] L. Martínez, R. Andrade, E.G. Birgin, J.M. Martínez, Journal of Computational Chemistry, 30 (2009) 2157-2164.

[41] S. Plimpton, Journal of Computational Physics, 117 (1995) 1-19.

[42] M. Salanne, P.A. Madden, Molecular Physics, 109 (2011) 2299-2315.

[43] B. Larsen, T. Førland, K. Singer, Molecular Physics, 26 (1973) 1521-1532.

[44] G. Kresse, J. Hafner, Physical Review B, 47 (1993) 558-561.

[45] G. Kresse, J. Furthmüller, Physical Review B, 54 (1996) 11169-11186.

[46] G. Kresse, D. Joubert, Physical Review B, 59 (1999) 1758-1775.

[47] S. Nosé, The Journal of Chemical Physics, 81 (1984) 511-519.

[48] J.P. Perdew, K. Burke, M. Ernzerhof, Physical Review Letters, 77 (1996) 3865-3868.

[49] J.P. Perdew, K. Burke, M. Ernzerhof, Physical Review Letters, 78 (1997) 1396-1396.

[50] J. Klimeš, D.R. Bowler, A. Michaelides, Physical Review B, 83 (2011) 195131.

[51] P.E. Blöchl, Physical Review B, 50 (1994) 17953-17979.

[52] C. Alexopoulos, in: Proceedings of the 38th conference on Winter simulation, Winter Simulation Conference, Monterey, California, 2006, pp. 168-178.

[53] F. Birch, Physical Review, 71 (1947) 809-824.

[54] F.D. Murnaghan, Proceedings of the National Academy of Sciences, 30 (1944) 244-247.

[55] D.C. Rapaport, The art of molecular dynamics simulation, Second Edition ed., Cambridge University Press, 2004.

[56] J.P. Perdew, A. Ruzsinszky, G.I. Csonka, O.A. Vydrov, G.E. Scuseria, L.A. Constantin, X. Zhou, K. Burke, Physical Review Letters, 100 (2008) 136406.

[57] G.J. Janz, Thermodynamic and transport properties for molten salts : correlation equations for critically evaluated density, surface tension, electrical conductance, and viscosity data, Published by the American Chemical Society and the American Institute of Physics for the National Bureau of Standards, New York, United States. , 1988.

[58] V.V. Ignat'ev, A.V. Merzlyakov, V.G. Subbotin, A.V. Panov, Y.V. Golovatov, At Energy, 101 (2006) 822-829.

[59] G.I. Csonka, J.P. Perdew, A. Ruzsinszky, P.H.T. Philipsen, S. Lebègue, J. Paier, O.A. Vydrov, J.G. Ángyán, Physical Review B, 79 (2009) 155107.

[60] S. Grimme, J. Antony, S. Ehrlich, H. Krieg, The Journal of Chemical Physics, 132 (2010) 154104-154119.

[61] S. Grimme, Journal of Computational Chemistry, 25 (2004) 1463-1473.

[62] S. Grimme, Journal of Computational Chemistry, 27 (2006) 1787-1799.

[63] M. Dion, H. Rydberg, E. Schröder, D.C. Langreth, B.I. Lundqvist, Physical Review Letters, 92 (2004) 246401.

[64] M.D. Grele, L. Gedeon, Forced-convection heat-transfer characteristics of molten Flinak flowing in an Inconel X system, National Advisory Committee for Aeronautics, Washington, DC, 1954.

[65] H.W. Hoffman, L. Jones, in, Oak Ridge National Laboratory Report ORNL-1977, 1955.

[66] D.T. Ingersoll, C.W. Forsberg, P.E. MacDonald, in, Oak Ridge National Laboratory Report ORNL/TM-2006/140, 2007.

[67] B. Vriesema, in, Thesis, Delft University of Technology, 1979.

[68] G.J. Janz, R.P.T. Tomkins, in, National Bureau of Standards Report NSRDS-NBS 61 Part IV, 1981.

[69] J. Garai, A. Laugier, Journal of Applied Physics, 101 (2007) 023514-023514.

[70] S. Cantor, J.W. Cooke, A.S. Dworkin, G.D. Robbins, R.E. Thoma, G.M. Watson, in, Oak Ridge National Laboratory, 1968.

[71] N. Iwamoto, Y. Tsunawaki, N. Umesaki, H. Ohno, K. Furukawa, Journal of the Chemical Society, Faraday Transactions 2: Molecular and Chemical Physics, 75 (1979) 1277-1283.

[72] T. Ohmichi, H. Ohno, K. Furukawa, The Journal of Physical Chemistry, 80 (1976) 1628-1631.

[73] N. Umesaki, N. Iwamoto, Y. Tsunawaki, H. Ohno, K. Furukawa, Journal of the Chemical Society, Faraday Transactions 1: Physical Chemistry in Condensed Phases, 77 (1981) 169-175.

[74] G.J. Janz, N.P. Bansal, Journal of Physical and Chemical Reference Data, 11 (1982) 505-693.

[75] W. Humphrey, A. Dalke, K. Schulten, Journal of Molecular Graphics, 14 (1996) 33-38.